Small-strain stiffness of the Pampeano Formation

Sfriso, A., Sagüés, P., Quaglia, G., Quintela, M. & Ledesma, O.
University of Buenos Aires

Keywords: Young's modulus, modulus reduction curve, LDT, Pampeano Formation, compacted soil

ABSTRACT: Buenos Aires, Argentina, rests on a loess deposit named Pampeano Formation. Foundations of buildings, industrial facilities, major infrastructure projects, metro tunnels and a nuclear power plant lay on this deposit. Pampeano soil is also used as a construction material for sub-bases, fills and embankments. A research program was established at the University of Buenos Aires to measure the small-strain nonlinear behavior of the material in the laboratory. A data acquisition system using LDTs was manufactured and installed in the triaxial apparatus, and a series of drained triaxial compression tests and one-dimensional compression tests was performed on both undisturbed and compacted samples. In this paper, the Pampeano Formation is briefly described, the data acquisition system is outlined, and some test results are presented. Data confirms the pressure dependency of the Young's modulus and modulus reduction curves for compacted samples and shows that undisturbed samples follow the same trend, a fact that was neither expected nor assumed in routine design due to the cementation of the material. Results obtained so far and the main objectives of future research work are discussed.

1 INTRODUCTION

Buenos Aires, the capital city of Argentina, lies on the so-called Pampeano Formation, which is a Pleistocene loess loam deposit formed by silts and clays heavily overconsolidated by dessication and erratically cemented with calcium carbonate (Arce 1968, Bolognesi 1959, Fidalgo 1975, Núñez 1986).

Foundations of buildings, industrial facilities, major infrastructure projects, metro tunnels and a nuclear power plant lay on this deposit. Large borrow pits are excavated to provide material for the construction of sub-bases, embankments and fills. Due to it's low cost and wide availability, most of the transportation network of Buenos Aires city is built on compacted Pampeano soils.

Despite the fact that Pampeano soils have been extensively used for the above mentioned purposes, little published information exists on the behavior of the material at small to intermediate strain, and no systematic effort has been done so far to measure the nonlinear stress-strain behavior of Buenos Aires soils in the laboratory.

This lack of information is partially compensated in practice by the selection of material parameters based on experience and back-analysis of the behavior of existing structures.

In 2007, a research program was established at the University of Buenos Aires to measure the mechanical properties of the deposit using both lab and field testing procedures.

The ultimate goal of this program is to establish practical correlations between key mechanical properties and some index parameters, namely void ratio and $CaCO_3$ content for undisturbed soils and compaction void ratio for compacted materials.

Although work is in progress, some preliminary results on the small-strain Young's modulus and constrained modulus of compacted Pampeano soils are available for public discussion and are presented in this paper.

2 THE PAMPEANO FORMATION

2.1 *Description*

The Pampeano Formation is a modified loess overconsolidated by dessication and cemented with calcium carbonate ($CaCO_3$) in nodule and matrix impregnation forms. This deposit forms the upper level of the stratigraphic profile of Buenos Aires city, reaching a depth of some 40 m at the center of

the city (Bolognesi 1959, 1975, Fidalgo 1975, Núñez 1986).

Soils of the Pampeano Formation plot close to the A line in the Casagrande chart, and classify either as ML, MH, CL or CH.

The deposit is very stiff. Except for the heaved upper three to six meters, penetration resistance is systematically $N_{SPT} > 20$ with some heavily cemented zones that exhibit very weak rock behavior with $N_{SPT} > 50$ (Nuñez 1986, Núñez and Micucci 1986).

2.2 *Geologic processes*

Silt and clay particles were transported by wind and water, and deposited under calm water, forming interbedded layers of fine materials of varying plasticity. Amorphous silica and volcanic ash particles were also deposited in quite heterogenous concentrations (Fidalgo 1975).

The reduction of the sea level associated to the last ice age lowered the water table and started a consolidation process. Intense droughts reduced the water content of the deposit that then became unsaturated and heavily overconsolidated by dessication (Bolognesi 1975, Núñez 1986).

Calcium carbonate and magnesium oxides precipitated during the drying process, bonding the particles together. Where the material was directly exposed to the arid climate, a pattern of fissures developed in the soil mass. Some of these fissures were afterwards sealed with calcium carbonate and other salts transported by rain infiltration (Bolognesi 1975, Núñez 1986).

The water table recovery and subsequent fluctuations saturated most of the soil mass. Restrained heave resulted in high lateral stresses, to the extent that the coefficient of earth pressure at rest is assumed to be in the range 0.7 – 1.0 (Núñez 1986, Sfriso 2006).

Three degrees of carbonate cementation can be distinguished (Núñez 1986, Núñez and Micucci 1986): i) nodules isolated in a non-cemented overconsolidated matrix; ii) an intermediate cemented matrix with strongly cemented nodules; and iii) the locally called "Tosca", a cemented matrix embedding very stiff calcium carbonate inclusions, the edges of these inclusions being readily distinguisable from the surrounding matrix.

2.3 *Shear strength*

The undrained unconfined compression strength of saturated, undisturbed samples depends on cementation and ranges from 300 kPa to 2000 kPa (Núñez and Micucci 1986).

Effective friction angles of the soils forming the upper part of the Pampeano formation are rather independent of cementation and are low bounded by the high pressure friction angle $\phi = 29º$ (Núñez and Micucci 1986, Núñez 2007). While friction angles up to 37° have been measured at low confining pressures, values above 32º are not used for design purposes (Sfriso 2006). An effective cohesion due to cementation is accounted for in practical engineering design. Despite the large uncertainty of the data and the highly erratic nature of carbonate cementation, a conservative value $c' \simeq 15kPa$ is used as an average property of the soil mass.

2.4 *In situ stiffness*

Reliable information of static in-situ stiffness is obtained with plate load tests performed in vertical shafts or pilot tunnels (Sfriso 2006). A primary loading modulus of subgrade reaction K and an unload-reload modulus K_{ur} are obtained in PLTs. K_{ur} can be used to estimate a pseudo-elastic modulus

$$E_{PLT} \simeq \tfrac{2}{3} \cdot K_{ur} \cdot B \qquad (1)$$

where B is the diameter of the plate. The typical in-depth variation of K, K_{ur} and E_{PLT} for Buenos Aires soils is listed in Table 1 (Sfriso 2008).

Table 1. In depth variation of PLT modulus of subgrade reaction and derived Young's modulus

Depth m	K MN/m^3	K_{ur} MN/m^3	E_{PLT} MPa
0 to 8/12	200 - 300	500 - 800	100 - 160
8/12 to 12/14	400 - 600	800 - 1200	160 - 240
12/14 to 20/24	600 - 800	1200 - 1800	240 - 360
20/24 to 30/32	250 - 500	600 - 1400	120 - 280

2.5 *Parameters for numerical modelling*

The hyperbolic model (Duncan and Chang 1970) implemmented as the HSM model in Plaxis (Schanz et al 1999) has been extensively used for the numerical analysis of underground constructions in Buenos Aires soils (Sfriso 1999, 2006). The set of material parameters for the HSM model that best fits the observed behavior of tunnels is listed in Table 2 (Sfriso 2008). The stress-strain relationships of the HSM model are reproduced in Eqns. (2a) to (2d) (Schanz et al 1999). It must be noted that exponent m of Eqns. (2c) and (2d) is set to 0 in Table 2.

Table 2. Material parameters used for numerical simulations of underground excavations

Depth (m):	0-8/12		8/12-20/24		>20/24	
	min	max	min	max	min	max
c_u (kPa)	50	100	110	220	40	120
ϕ_u (°)	10	20	5	20	0	5
c' (kPa)	10	25	25	50	15	30
ϕ' (°)	28	31	30	34	28	31
ψ (°)	0	3	0	6	0	3
E_{50}^{ref} (MPa)	60	100	75	150	60	100
E_{ur}^{ref} (MPa)	150	250	180	300	140	220
m (-)	0	0	0	0	0	0
ν (-)	0.20	0.30	0.20	0.30	0.25	0.35
R_f (-)	0.80	0.90	0.80	0.90	0.80	0.90

$$\sigma_1 - \sigma_3 = \begin{cases} \text{load: } 2E_{50}\left(1 - R_f \dfrac{\sigma_1 - \sigma_3}{\sigma_3 N_\phi + 2c\sqrt{N_\phi}}\right)\varepsilon_1 \\ \text{unload: } E_{ur}\varepsilon_1 \end{cases} \quad (2a)$$

$$N_\phi = \tan^2\left[\frac{\pi}{4} + \frac{\phi}{2}\right] \quad (2b)$$

$$E_{ur} = E_{ur}^{ref}\left(\frac{\sigma_3 + c\cot[\phi]}{c\cot[\phi] + p_{atm}}\right)^m \quad (2c)$$

$$E_{50} = E_{50}^{ref}\left(\frac{\sigma_3 + c\cot[\phi]}{c\cot[\phi] + p_{atm}}\right)^m \quad (2d)$$

In Eqns. (2a) to (2d) and Table 2, σ_1 and σ_3 are the major and minor principal stresses, ε_1 is the major principal strain, c is either the undrained cohesion c_u or drained cohesion c', ϕ is either the undrained friction angle ϕ_u or drained friction angle ϕ', ψ is the dilatancy angle, E_{50}^{ref} and E_{ur}^{ref} are the reference loading and un/reloading Young's moduli, m is an exponent controlling the dependence of stiffness on stress state, ν is the Poisson's ratio, R_f is the failure ratio and p_{atm} is atmospheric pressure (Schanz et al 1999).

3 EXPERIMENTAL PROGRAM

3.1 *Program outline*

The small-strain Young's modulus and modulus reduction curve of both undisturbed and compacted samples was measured in triaxial compression staggered tests with local deformation measurement using LDTs. Six undisturbed samples and five compacted samples were tested at five confining pressures.

Two series of one dimensional compression tests were also performed on undisturbed and compacted samples to measure the constrained modulus. One consolidation test of a slurry sample was also performed for comparison purposes.

3.2 *Triaxial apparatus*

The triaxial apparatus used is composed by a load frame, a triaxial cell and a data acquisition system.

The load frame is a deformation controlled Wykeham-Farrance mechanical device with a load capacity of 25 kN. The deformation rate can be selected in the range 1.2 to 7500 μm/min by adjustment of a 30 positions gearbox.

The triaxial cell has a capacity of 7250 cm^3. It can test cylindrical samples in the range 76 – 101 mm dia and 100 – 200 mm high with cell pressures in the range 0 – 800 kPa. Air is used as cell fluid. A 10 kN x 10 N load cell is used for the axial load. To eliminate the effect of the piston friction, the load cell is located inside the test chamber.

Two conventional LDTs, 90 mm long, were employed to measure axial deformation (Goto 1991). LDT's accuracy requires the temperature of the strain gauges to remain fairly constant throughout the test. Although this objective is not attainable because the current passing through the strain gauges heates the clips, the effect was minimized by employing full Wheatstone bridges in each LDT. This configuration also improves the instrument accuracy when compared to a single strain gauge clip (Dasari 1995).

Radial deformation was measured with three cantilever LDTs fixed to the chamber base as shown in Fig. 1.

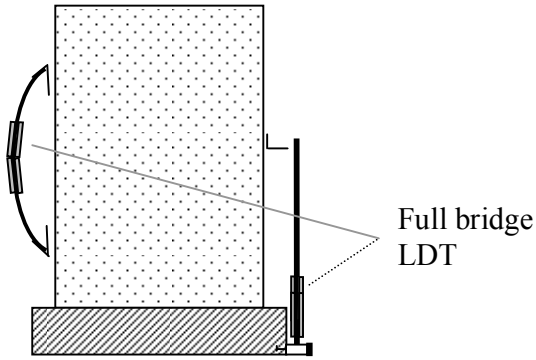

Figure 1. Full bridge axial and radial LDTs.

Due to this configuration, radial LDTs measure absolute radial displacement at three points of the sample instead of changes in diameter. LDTs were calibrated with a mechanical micrometer and used within one half of the measured elastic range. The measured working range of the axial LDTs is 5 mm x 2 μm, while for the radial LDTs the working range is 6 mm x 4 μm. Fig. 2 shows a sample mounted on the triaxial cell.

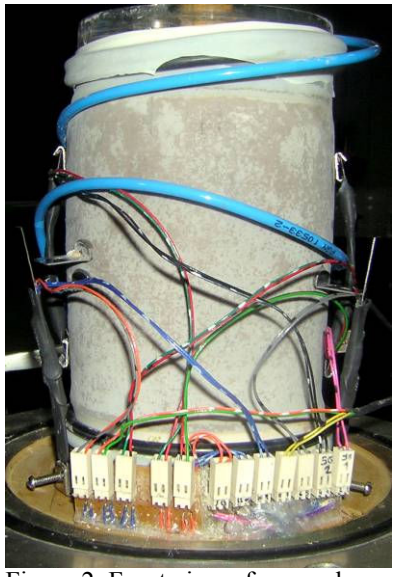
Figure 2. Front view of a sample mounted on the triaxial cell.

Inexpensive Emant 300 data acquisition modules with strain application adaptors were employed to capture the load cell data and to read all the LDTs simultaneously.

3.3 *Testing of undisturbed samples*

Undisturbed samples were obtained at a large underground cavern named "Estación Corrientes" which is part of the expansion of Metro Line H (Sfriso 2007).

Thin walled 101 mm steel tubes were driven into the soil by static pressure applied by a backhoe excavator. The tubes were then removed, sealed with polyethilene film and transported to the lab. All samples were tested within 48 hours after extraction.

Samples for triaxial compression were saturated in the tube samplers for 48 hours and statically pushed out after saturation. The saturation procedure used was upwards flooding enhanced by vacuum application at the upper face of the sample. A porous stone kept the upper face of the samples confined to prevent and sample disturbance due to the high pore pressure gradients applied.

The physical properties of the undisturbed samples tested fall in the following ranges: unit weight of solid particles γ_s = 26.1 – 26.8 kN/m^3; liquid limit ω_L = 44% – 56%; plasticity index I_P = 15% – 23%; 84% – 96% finer than #200 sieve, 12% – 23% of particles smaller than 2μm and a $CaCO_3$ content 0.2% – 2.5%.

The index parameters of the samples tested in triaxial compression are shown in Table 3. Notation is as follows: ω_i is the natural moisture content, ω_f is the moisture content after saturation, γ_d is the dry unit weight, $CaCO_3$ is the carbonate content, k is the saturated permeability and B is the Skempton parameter. Additional saturation was performed in the triaxial cell when the samples failed to accomplish with a B>0.95. All samples were 101 mm dia and trimmed to a height 127 mm +/- 1 mm.

In each of the five stages the samples were loaded to a stress ratio σ_1/σ_3 = 2.0 and unloaded to zero deviatoric stress before the cell pressure was increased and the next stage was performed. The loading rate was 0.4 mm/hr for all tests.

One dimensional compression tests were performed directly in the tube samplers after saturation and trimming to an approx. 1:5 height to diameter ratio. The index properties of the samples tested in 1D compression are shown in Table 4, where h is the height of the sample and e is the initial void ratio. Tests were performed at one stage/day.

Table 3. Properties of undisturbed samples tested in triaxial compression.

	ω_i %	ω_f %	γ_d kN/m^3	$CaCO_3$ %	k m/s	B -
UT1	32.0	32.8	13.60	2.1	5.3·E-7	0.96
UT2	33.2	34.0	12.50	2.2	6.7·E-7	0.95
UT3	37.7	38.8	14.10	1.0	4.5·E-7	0.98
UT4	27.2	27.8	14.60	0.2	1.9·E-6	0.97
UT5	27.0	28.0	14.40	0.4	2.0·E-6	0.98
UT6	27.5	28.7	14.20	0.3	1.2·E-6	0.96

Table 4. Properties of undisturbed samples tested in one dimensional compression

	ω_i %	γ_d kN/m^3	h mm	$CaCO_3$ %	e
UC1	41.2	13.59	25.90	2.1	1.27
UC2	28.1	14.14	21.59	2.1	1.07
UC3	32.0	13.59	22.00	2.5	1.12
UC4	34.3	14.35	21.52	2.4	1.24
UC5	32.6	13.82	22.10	2.2	1.39
UC6	27.1	14.11	24.02	1.0	0.98

3.4 *Testing of compacted samples*

Compacted samples were prepared from a batch of low plasticity silt taken from a commercial borrow pit located about 30 km south of Buenos Aires City.

The physical properties are: unit weight of solid particles γ_s = 26.8 kN/m^3; liquid limit ω_L = 45%; plasticity index I_P = 9%; 90.2% finer than #200 sieve and a 17% of particles smaller than 2μm. As per ASTM D698 Method A, the optimum water content is ω_{op} = 28.7% and the max dry density is γ_d =14.3 kN/m^3. A swelling index of 2.26% and a saturated permeability k = 4.1·10^{-8} m/s were measured at samples compacted at the optimum water content.

Air dried material was moisted to the selected water content and stored for 48 hours to allow for moisture homogeneization. Triaxial test samples were made by impact compaction in the standard 101 mm compaction mold following ASTM D-698 Method A test procedure, and saturated for 48 hours before removal from the mold.

The index properties of the samples tested in triaxial compression are shown in Table 5. Notation is as follows: ω_c is the compaction moisture content, γ_d is the compacted dry unit weight, S_r is the saturation ratio after compaction, ω_i is the moisture content after saturation. Additional saturation was performed when the samples failed to accomplish with a B>0.95. The loading rate was 0.1 mm/hr for all tests.

Samples for the one dimensional compression tests were compacted directly in consolidation rings attached to the compaction mold and saturated under a low vertical pressure of 5 kPa. It was observed that the samples ceased to heave after approx. 48 hours and this was used as an indicator of full saturation. The samples were then trimmed to an approx. 1:5 height to diameter ratio and tested at one stage/day.

Table 5. Properties of compacted samples tested in triaxial compression.

	ω_c °%	γ_d kN/m^3	e -	S_r %	ω_i %	k m/s	B -
CT1	24.5	13.7	0.96	69	35.5	6.9·E-8	0.97
CT2	26.5	14.0	0.91	77	34.3	5.1·E-8	0.97
CT3	28.7	14.3	0.87	88	32.5	4.1·E-8	0.96
CT4	30.1	14.0	0.91	88	34.4	3.0·E-8	0.95
CT5	30.3	13.9	0.93	87	34.9	3.2·E-8	0.96

The index properties of the samples tested in one dimensional compression are shown in Table 6. Notation is as follows: compaction effort (for the 101 mm mold) is given in (no. of blows x hammer mass x drop height), h is the height of the sample after compaction and trimming and δ is the total heave during saturation stage. It can be seen that samples CC5 and CC6 exhibited large heave associated to the higher compaction efforts applied.

Table 6. Properties of compacted samples tested in one dimensional compression.

	Compaction n° x kg x m	ω_c %	γ_d kN/m^3	ω_i %	h mm	δ %
CC1	slurry	47.3	11.82	47.3	15.51	0.0
CC2	15x2.5x0.30	27.8	12.21	42.9	24.71	0.5
CC3	25x2.5x0.30	28.2	14.13	34.1	18.64	2.3
CC4	25x2.5x0.30	23.9	13.08	39.6	20.25	2.5
CC5	25x5.0x0.45	22.0	14.53	37.7	20.55	3.6
CC6	25x5.0x0.45	27.2	14.54	35.1	19.91	3.0

4 RESULTS

4.1 *Small-strain Young's modulus*

The small-strain Young's modulus E_{max} is defined as the initial modulus at primary loading and is assumed to be equal to the un/reload modulus E_{ur} obtained in a small unload-reload cycle.

For compacted samples, E_{ur} was measured at small unload-reload cycles after the samples were deformed monotonically to an axial strain $\varepsilon_a = 10^{-4}$.

For undisturbed samples, E_{ur} was measured in primary loading at a reference axial strain $\varepsilon_a = 10^{-5}$, which is close to the precision of the available measurement devices. This procedure was preferred because damage of cementation was expected to occur at an axial strain $\varepsilon_a = 10^{-4}$. Fig. 3 shows E_{ur} for the six undisturbed samples and five compacted samples tested at five confining pressures.

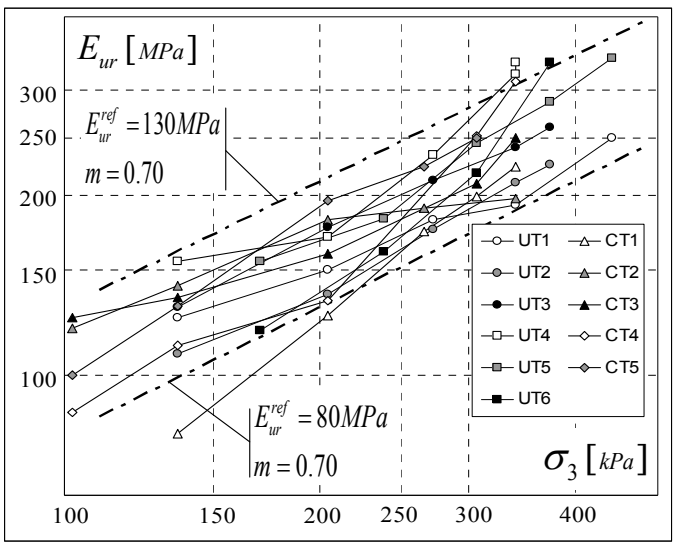

Figure 3. Small-strain Young's modulus dependence on cell pressure. Data from 6 undisturbed and 5 compacted samples.

It can be noticed that E_{ur} depends on cell pressure for both undisturbed and compacted samples.

Parameters of Eqn. (2c) may be calibrated after this information if c = 0 kPa. is adopted. A lower bound E_{ur}^{ref} = 80MPa, an upper bound E_{ur}^{ref} = 130 MPa and an unexpectedly high exponent m = 0.7 are found to fit the obtained data.

The amount of information is not enough to establish a general trend: the strong dependence of the small-strain modulus on confining pressure could be a true material property, reflect disturbance associated to tube sampling of cemented soils or respond to the well-known existence of fissures in the soil mass. This subject deserves further investigation.

4.2 *Small- strain Poisson's ratio*

A fairly constant Poisson's ratio in the range 0.15 – 0.18 has been obtained for all tests and load stages. No dependency has been found so far between the Poisson's ratio, cell pressure and compaction void ratio.

4.3 *Modulus reduction curves*

The secant Young's modulus is defined as

$$E_s = \sigma_d / \varepsilon_a \tag{3}$$

where $\sigma_d = \sigma_1 - \sigma_3$ is the effective stress difference and ε_a is total axial strain. The hyperbolic law (Hardin and Richart 1963) relates the secant modulus E_s with the most elastic modulus E_{ur} through the expression

$$E_s = E_{ur} / \left(1 + \varepsilon_a / \varepsilon_r\right) \tag{4}$$

where ε_r is a parameter that can be obtained from a E_s/E_{ur} vs. ε_a plot as the abcisa where E_s/E_{ur} = 1/2. Results are shown in Fig. 4 for all tests and stages. It can be noticed that $10^{-4} < \varepsilon_r < 10^{-3}$ for compacted samples and $\varepsilon_r > 10^{-3}$ for undisturbed samples.

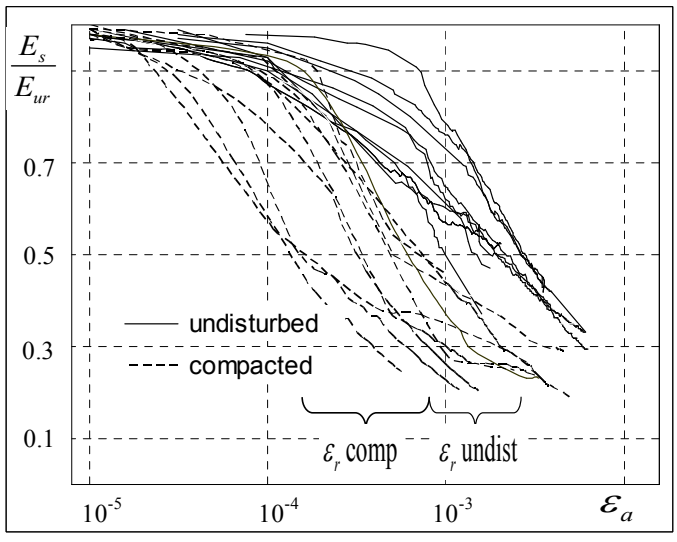

Figure 4. Modulus reduction curves for compacted (dashed lines) and undisturbed (solid lines) samples .

4.4 *Static Young's modulus*

A Young's modulus representative of the overall behavior of the material under static loading is frequently required for design purposes. For undisturbed soils, the static Young's modulus can be estimated with the information given in Table 1. For compacted soils, a modulus E_0 representative of static loading can be defined as the secant Young's modulus at a deformation $\varepsilon_a = 5 \cdot 10^{-4}$, which is an average value for ε_r. Fig. 5 shows both E_0 and E_{ur} for the five compacted samples tested, along with the fitting equation (Janbu 1963)

$$E_0 = 45\left(\frac{\sigma_3}{100kPa}\right)^{0.55} MPa \qquad (5)$$

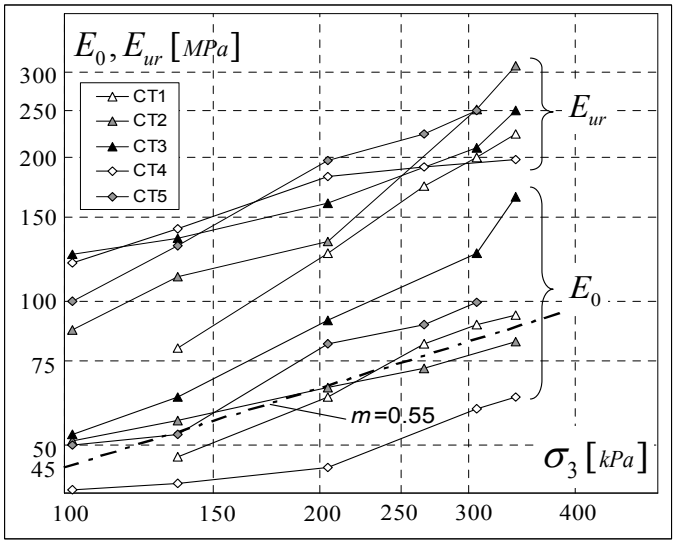

Figure 5. E_0 and E_{ur} as a function of cell pressure for compacted samples.

4.5 *Constrained unload/reload modulus*

One dimensional compression tests are shown in Fig. 6 for undisturbed samples and in Fig. 7 for compacted samples. While undisturbed samples showed almost elastic behavior when unloaded, compacted samples swelled slightly.

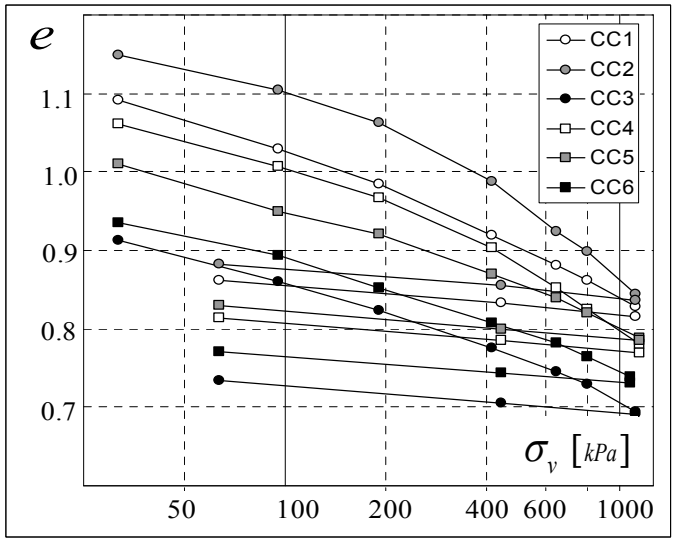

Figure 6. 1D compression of undisturbed samples.

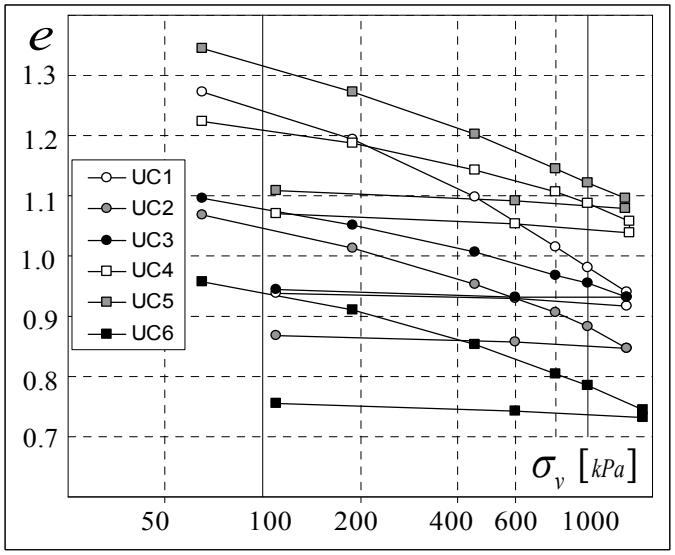

Figure 7. 1D compression of compacted samples.

Fig. 8 shows the recompression index of both undisturbed and compacted samples as a function of void ratio.

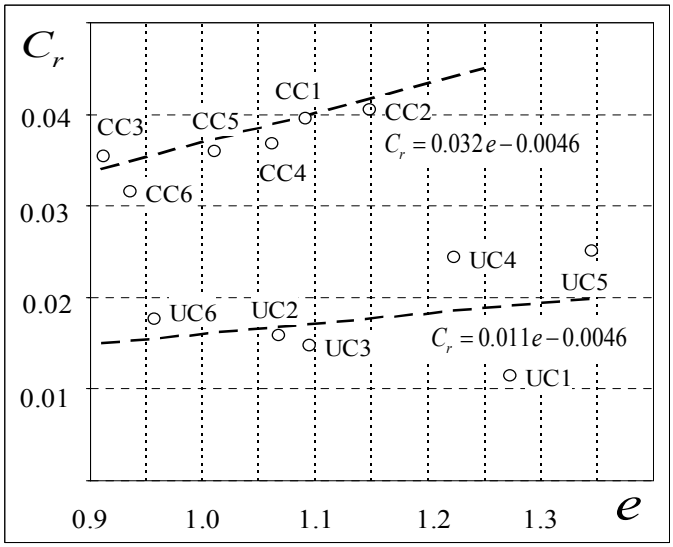

Figure 8. Recompression index of undisturbed and compacted samples as a function of void ratio.

Best fit equations for the recompression index are

$$C_r = 0.011e - 0.0046 \qquad (6)$$

for undisturbed samples and

$$C_r = 0.032e - 0.0046 \qquad (7)$$

for compacted samples. It is concluded that C_r for undisturbed samples is roughly one half that of samples compacted to the same void ratio.

The unload/reload constrained modulus

$$E_{oed} = \partial\sigma_v / \partial\varepsilon_1 \qquad (8)$$

is a useful design parameter for pavement engineering. E_{oed} is related to C_r through the well-known expression

$$E_{oed} = 2.3(1+e)\sigma_v / C_r \qquad (9)$$

The fact that C_r is a function of void ratio implies that E_{oed} is a nonlinear function of vertical stress and void ratio. For instance, sample CC3 (100% Proctor ASTM 698 Method A), tested at primary loading at σ_v = 100 kPa (e = 0.87) yields a constrained modulus

$$E_{oed} = \frac{2.3 \cdot (1 + 0.87)}{0.032 \cdot 0.87 - 0.0046} 100kPa = 18.5MPa \quad (10)$$

The same material consolidated to σ_v = 1050 kPa and unloaded to σ_v = 100 kPa (e = 0.72), yields

$$E_{oed} = \frac{2.3 \cdot (1 + 0.72)}{0.032 \cdot 0.72 - 0.0046} 100kPa = 21.5MPa \quad (11)$$

It must be recalled that C_r includes swelling, if any, and therefore E_{oed} can neither be regarded as an elastic material parameter nor be compared with E_{ur}.

4.6 *Preconsolidation vertical stress*

For compacted samples, the effect of increasing compaction energy is not the development of an apparent preconsolidation vertical stress (i.e. a yield stress) but an increase in the constrained modulus and a reduction in the compression index. Although it is assumed that all curves join at some point beyond the capacity of the consolidation apparatus, it is evident that plastic deformations develop for primary loading, irrespective from the compaction effort and compaction void ratio. Undisturbed samples show a similar trend.

Fig. 9 puts together the results of the two series of one dimensional compression tests in a normalized plot where $\Delta e = e - e_i$ is used in the vertical axis to remove the effect of varying initial void ratios.

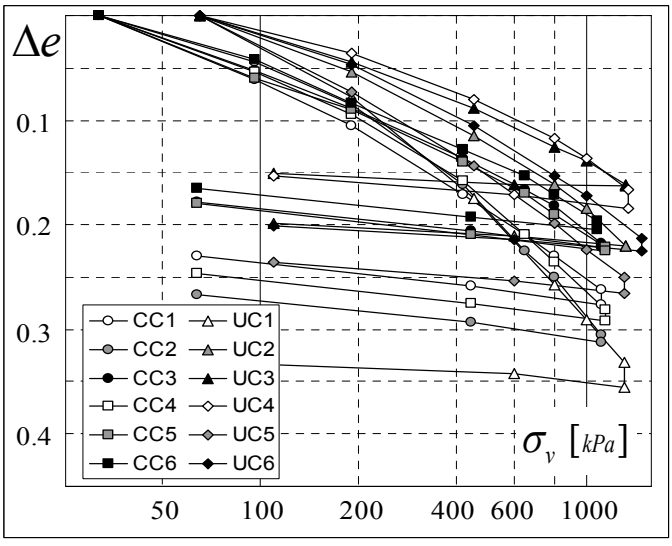

Figure 9. Normalized plot of all 1D compression tests. Scatter is very low for compacted samples and high for undisturbed samples.

It is observed that compacted samples have almost identical curves irrespective of compaction effort and initial void ratio.

On the other hand, undisturbed samples show a high degree of scatter, a fact that can be attributed to spatial variability of void ratio, carbonate cementation and stress history.

5 CONCLUSIONS

A research program on the Pampeano Formation has been established at the University of Buenos Aires. As part of this program, a series of triaxial compression tests and one dimensional compression tests were performed on compacted and undisturbed samples of Pampeano soils. The equipment used and some available results to date are presented.

The Pampeano Formation is an overconsolidated loess loam cemented with calcium carbonate and fissured due to strong dessication. Stiffness parameters used in practice are largely based on experience, as no systematic effort has been done so far to measure the nonlinear stress-strain behavior of Buenos Aires soils in the laboratory. For numerical modelling, the common practice is to disregard the pressure dependency of the Young's modulus and modulus reduction curves and to adopt a small-strain Young's modulus independent of stress level.

Results shown in this paper differ from this assumed behavior. The small-strain Young's modulus has been found to strongly depend on confining pressure for undisturbed samples. Moreover, it has been found that the modulus dependency on confining pressure is similar for undisturbed and compacted samples.

The information is not enough to establish a general trend, as uncertainties remain with respect to sample disturbance and the effect of the pre-existing fissures in the soil mass, so the topic deserves further investigation.

The recompression index and the constrained unload-reload modulus were also measured for both undisturbed and compacted samples. It was observed that the recompression index of undisturbed samples is roughly one half that of samples compacted to the same void ratio. Further investigation is needed to verify and extend the validity of these findings.

ACKNOWLEDGEMENTS

Much of the results presented here have been produced by the junior authors as part of their undergraduate thesis projects at the LMS, University of Buenos Aires. Dycasa SA, the company which builds Estación Corrientes, provided the means and permissions to acquire undisturbed samples and to publish the results. Prof. Eduardo Núñez discussed some of the results with the senior author. The contribution of the individuals working in these organizations is gratefully acknowledged.

REFERENCES

Arce, C., Médici, J. and Salles, M. (1968). "Condiciones geotécnicas y fundaciones adoptadas en algunas obras del bañado de Flores", 1st RAMSIF, La Plata, 347-380.

Bolognesi, A. and Moretto, O. (1959). "Propiedades del subsuelo del Gran Buenos Aires", 1st CPMSC, I, 303-314.

Bolognesi, A. (1975). "Compresib de los suelos Formación Pampeano ", V PCSMFE, Argentina, V: 255-302.

Dasari, G., Bolton, M., and Ng, C. (1995). "Small strain measurement using modified LDTs", Report CUED/D-SOILS/TR275, Geotech. Group, Cambridge University.

Duncan, J. and Chang, C. (1970). "Nonlinear analysis of stress and strain in soils ", Journal of Soil Mechanics Foundation Division, ASCE, 96, SM5, 1629-1653.

Duncan, J., Byrne, P., Wong, K., and Mabry, P. (1980). "Strength, stress-strain and bulk modulus parameters for finite element analyses of stresses and movements in soil masses ", Report UCB/GT/80-01, Berkeley, 72 p

Fidalgo, F., De Francesco, F. and Pascual, R. (1975). "Geología superficial de la llanura Bonaerense", VI Arg. Geol. Conf, 110 - 147.

Goto, S., Tatsuoka, F., Shibuya, S., Kim, Y. and Sato, T. (1991). "A simple gauge for local small strain meas. in laboratory", Soils and Found. 31, 1, 169-180.

Janbu, N. (1963). "Soil compressibility as determines by oedometer and triaxial tests", Proc. Eur. Conf. Soil Mech. Found. Eng., Wiesbaden, I, 19-25.

Hardin, B. and F. Richart (1963). "Elastic wave velocities in granular soils ", JSMFD, ASCE, 89, SM1, 33-65.

Núñez, E. (1986). "Panel Report: Geotechnical conditions in Buenos Aires City", V Int. Conference IAEG, 2623-2630.

Núñez, E. and C. Mucucci (1986). "Cemented preconsolidated soils as very weak rocks", V Conference IAEG, 403-410.

Núñez, E. (2007). "Casagrande lecture: Uncertainties and Approximations in Geotechnics", XIII PCSMGE, Venezuela, pp. 1 – 17.

Schanz, T., Vermeer, P. and Bonnier, P. (1999). "The hardening soil model: formulation and verification". Proc Plaxis Symp Beyond 2000 in Computational Geotechnics Amsterdam, Balkema, pp. 55-58.

Sfriso, A. (1999). "Tunnels in Buenos Aires: Application of numerical methods to the structural design of linings", XI PCSMGE, 637-642.

Sfriso, A. (2006). "Algunos proc. constructivos para la ejecución de túneles urbanos", XIII CAMSIG, San Juan.

Sfriso, A. (2007). "Procedimiento Constructivo de la Estación Corrientes del Subterráneo de Buenos Aires, Argentina". VI Chilean Conf. Geot. Eng., 124-132.

Sfriso, A. (2008). "Metro tunnels in Buenos Aires: Design and construction procedures 1998 – 2007", Sixth Int. Symp. Geot. Aspects Underground Constr. in Soft Ground (IS-Shanghai 2008), In press.